(DOI will not work until issue is live.) DOI: http://dx.doi.org/10.2138/am.2014.4463

The sound velocity measurements of Fe_3S

Revision 1

Seiji Kamada[1,2,*], Eiji Ohtani[1], Hiroshi Fukui[3,4], Takeshi Sakai[1], Hidenori Terasaki[1,5], Suguru Takahashi[1], Yuki Shibazaki[1], Satoshi Tsutsui[6], Alfred Q. R. Baron[3,6], Naohisa Hirao[6], and Yasuo Ohishi[6]

1: Department of Earth and Planetary Materials Science, Graduate School of Science, Tohoku University, Sendai, 980-8578, Japan.

2: Department of Geology, University of Illinois at Urbana-Champaign, 1301 West Green street, Urbana, IL, 61801.

3: Materials Dynamics Laboratory, RIKEN SPring-8 Center, 1-1-1 Kouto, Sayo 679-5148, Japan.

4: Graduate School of Material Science, University of Hyogo, 3-2-1, Kamigori, Hyogo 678-1279, Japan.

5: Department of Earth and Space Science, Graduate School of Science, Osaka University, Osaka 560-0043, Japan.

6: Japan Synchrotron Radiation Research Institute, Sayo, Hyogo 679-5198, Japan.

*: corresponding author

Abstract

We measured the sound velocity of Fe_3S at room temperature up to 85 GPa employing inelastic X-ray scattering in order to better constrain the constitution of the inner core. The density of Fe_3S was also determined by X-ray diffraction under the same conditions. The relation of the P-wave velocity (V_P) and density (ρ) of

Fe_3S follows Birch's law, V_P[m/s] = 1.14(5) × ρ[kg/m^3] − 2580(410). Based on Birch's law determined here for Fe_3S and that for ε-Fe reported previously, we found that sulfur decreases both density and compressional velocity of hcp-Fe at the core pressure and 300 K.

Keyword: Fe_3S, inner core, sound velocity, Birch's law, inelastic X-ray scattering.

Introduction

The Earth's core has been studied seismologically, and seismic wave velocities and the density of the core are important observable properties (e.g., Birch 1964; Dubrovinsky et al. 2000). According to these studies, the inner core is less dense than pure iron, and it has been accepted that the inner core is comprised of iron and light elements (e.g., Poirier 1994). Sound velocity data are more accurate than density in seismology and can provide important constraints on the structure and composition of the inner core (e.g., Badro et al. 2007; Cao et al. 2005; Song and Helmberger 1998). In spite of their importance, the sound velocity data of the core materials at high pressure are still very limited due to technical difficulties although many experiments to constrain the density of the inner core have been carried out using in situ X-ray diffraction (e.g., Chen et al. 2007).

Sulfur has been suggested as one of the most plausible light elements in the Earth's core (e.g., Campbell et al. 2007; Seagle et al. 2006). The S content in the core is estimated to be at least a few weight per cent (Hillgren et al. 2000; McDonough 2003). In previous work, phase relationships in the Fe–FeS system under high pressures were investigated (e.g., Fei et al. 2000; Kamada et al. 2010). Kamada et al. (2010) confirmed that Fe_3S is stable with ε-Fe up to 220 GPa, and Fe_3S is therefore one of the candidates of the inner-core materials. The compression behavior of Fe_3S was investigated up to 80 GPa (Seagle et al. 2006; Chen et al. 2007). Chen et al. (2007) estimated the S content to be 12.5–20.7 at% (7.9–13.0 wt%) in the outer core and 2.2–6.2 at% (1.4–3.7 wt%) in the inner core. Other studies have investigated the sound velocities, V_P, of iron and iron–light-element alloys (e.g., Antonangeli et al. 2004; Badro et al. 2007; Fiquet et al. 2001). Although sound velocities of FeS and FeS_2 have been measured according to inelastic X-ray scattering (IXS), there are very limited data for Fe_3S. FeS and FeS_2 may not be appropriate for the inner core materials because the Fe–S system has several iron-rich intermediates such as Fe_3S_2, Fe_2S, Fe_3S coexisting with Fe and high pressure polymorphs in FeS at high pressure (Fei et al. 1995). Only Fe_3S coexists with ε-Fe under the core conditions as a subsolidus phase (Kamada et al. 2010, 2012). Therefore, it is essential to study V_P of Fe_3S to understand the seismic and chemical properties of the Earth's core. Lin et al. (2004) studied V_P of Fe_3S up to 57 GPa employing NIS (Nuclear Resonance Inelastic X-ray scattering) and found that it follows Birch's law, which suggest the linear relationship between density and sound velocity (Birch 1961). They also reported that the sound velocity of Fe_3S changes significantly across the magnetic transition occurred at approximately 21 GPa. However the application of the results to the earth's core was not made due to a narrow pressure interval of their NIS measurements. In this research, we measured V_P of Fe_3S based on inelastic X-ray scattering method up to 85 GPa.

Experimental method

The starting material of Fe_3S was synthesized by a multianvil press from a mixture of powdered Fe (99.9% purity) and FeS (99.9% purity) with the ratio of Fe:S = 85:15 (wt%). The synthesis conditions were 21 GPa and temperatures between 1263 K and 1553 K. The sample was first compressed to 21 GPa at room temperature and then heated above the melting temperature at 1533 K for 5 min to homogenize the mixture. The temperature was then lowered to 1413 K and kept at that temperature for 30 min to crystallize Fe_3S from the Fe–S liquid. The temperature was then reduced to 1263 K and kept at that temperature for 1 h for the growth of the Fe_3S crystals. The chemical composition of the recovered sample was determined to be $Fe_{73.4(0.1)}S_{26.6(0.1)}$ (in at%) using a scanning electron microscope with energy dispersive X-ray spectroscopy and its bask scattered image is shown in Figure 1. A small fragment of the recovered sample was used for inelastic X-ray scattering (IXS) experiments at high pressures.

A symmetric diamond anvil cell was used to generate high pressure. The culet sizes of the diamond anvils were 200, 350, and 400 μm, respectively. A sample was loaded into the hole of a pre-indented rhenium gasket, which was typically about 50 μm thick. The diameter of the sample chamber was 60–100 μm. The sample was sandwiched between NaCl pellets, which served as the pressure-transmitting medium, a thermal insulator, and a pressure scale. A double-sided laser heating method using fiber lasers was used for annealing. The sample was compressed to the target pressure at room temperature, and then annealed at around 1500–2000 K depending on each experimental pressure at BL10XU of SPring-8, Japan (Ohishi et al. 2008). After annealing, XRD patterns were taken at the beamline BL10XU, SPring-8. The diameter of the X-ray beam was collimated to be 15 μm. The typical X-ray wavelength used was 0.41348(7) Å. An imaging plate was used as an X-ray detector. The typical exposure time was 10 min. Each integrated X-ray profile along with the 2θ angle was analyzed using the WinPIP software package (Fujihisa 1999, 2005; Fujihisa and Aoki 1998), and the PD Indexer software package (Seto et al. 2010) and the existence of Fe_3S and absence of other impurities were confirmed in all starting samples for the present high-pressure experiments. The density of Fe_3S was measured for the same high pressure cell assembly before or after each IXS measurement using X-ray diffraction (XRD) for the same samples at BL10XU, SPring-8. The pressure was determined from the equation of states (EOS) of NaCl B1/B2 phases (Fei et al. 2007; Matsui et al. 2009).

IXS experiments were performed at BL35XU, SPring-8, Japan (Baron et al. 2000). The sample was placed in the diamond anvil cell which was set, in a helium gas atmosphere, on the Eulerian cradle of the IXS spectrometer. Focusing with a pair of Kirkpatrick–Baez mirrors reduced the beam size to about 15 μm vertically by 17 μm horizontally (full width at half maximum). The energy resolution was 3.0 meV FWHM at 17.795 keV using the Si (999) reflection. A 3 × 4 array of spherical analyzer crystals was set at the end of the 10-m horizontal arm to analyze the scattered X-rays with 12 different scattering vectors. Energy scans at constant momentum transfer were carried out by varying the energy of the X-rays incident on the sample. The momentum resolution was set by slits in front of the analyzers to about 0.38–0.41 nm^{-1}, full width. Each set of spectra was collected for 8–10 h. The Stokes scattering contributed by LA phonons was fitted with a Lorentzian function to obtain the energy position at each momentum transfer, *Q*. Using the 12-crystal analyzers, we can obtain the relationship between momentum transfer and energy of acoustic phonons across the first Brillouin zone. Because polycrystalline Fe_3S was used as a sample, the V_P measured was orientation-averaged.

Results and discussion

The IXS from Fe_3S was measured in the pressure ranging from 23.8 to 84.5 GPa. The experimental conditions and results are summarized in Table 1. Examples of IXS spectra at different pressures and their fitting results are shown in Figure 2. The peak observed at zero energy in each spectrum relates to elastic scattering from the sample. Open diamonds represent peak positions of transverse acoustic (TA) phonons from a diamond anvil. Because diamond has high sound velocities, TA phonon peaks were observed at higher energy and only low Q conditions. Solid diamond symbols represent peak positions of LA phonons of Fe_3S. Each peak energy position was obtained by fitting a Lorentzian function to the peak.

Each dispersion relationship between energy and momentum transfers was fitted using eq. (1), and the dispersion curves obtained are shown in Figure 3.

$$E[\mathrm{meV}] = 4.192 \times 10^{-4} V_P[\mathrm{m \cdot s^{-1}}] \times Q_{MAX}[\mathrm{nm^{-1}}] \times \sin\left[\frac{\pi}{2}\frac{Q[\mathrm{ns^{-1}}]}{Q_{MAX}[\mathrm{ns^{-1}}]}\right], \qquad (1)$$

where E and Q are the energy and momentum transfers to the phonon and V_P is the sound velocity of the sample. V_P and Q_{MAX} are free parameters. The results are summarized in Table 1. The energy of the Fe_3S LA phonon at the same Q increases with increasing pressure, indicating that V_P increases with increasing pressure.

The results of this study are plotted as a function of density in Figure 4 together with results from previous studies. The compressional velocity and density of the inner core for the preliminary reference Earth model (PREM) (Dziewonski and Anderson 1981) are also plotted in this figure. The present data are plotted in the figure together with previous studies. The slopes of Birch’s law decrease with decreasing the amount of sulfur in iron sulfides. The slope of Fe_3S is similar to that of Fe. The present velocities are consistent with those of Lin et al. (2004) and follow Birch's law (Birch 1961) as shown in Figure 4. The linear relationship between density and sound velocity was obtained by combining the data from the present study with those from Lin et al. (2004),

$$V_P[\text{m/s}] = 1.14(5) \times \rho[\text{kg/m}^3] - 2580(410) \quad \left(R^2 = 0.983\right), \qquad (2)$$

where ρ is the density of Fe_3S.

Theoretical calculations using the *ab initio* method (Sha and Cohen 2010; Vočadlo et al. 2009) revealed a large temperature effect on Birch's law above 2,000 K. Recent IXS measurement of ε-Fe (Antonangeli et al. 2012; Mao et al. 2012) revealed that the density–V_P relation significantly deviates from the shock compression data suggesting a large temperature dependency of Birch's law, although the effect of temperature is negligible in the lower temperature range. V_P and density of hcp-Fe measured at 300 K (Antonangeli et al. 2012; Mao et al. 2012) and calculated theoretically (Sha and Cohen 2010; Vočadlo et al. 2009) at 0 K provide Birch's law for hcp-Fe as follows:

$$V_P[\text{m/s}] = 1.18(4) \times \rho[\text{kg/m}^3] - 3660(430) \quad \left(R^2 = 0.986\right). \qquad (3)$$

Comparing with equations (2) and (3), we can evaluate the effect of sulfur in Birch's law for hcp-Fe at 300 K. Figure 4 shows the density and compressional velocity of Fe_3S and hcp-Fe at the core pressures of 136 GPa and 330 GPa at 300 K. This figure clearly indicates that both density and compressional velocity of Fe_3S at 300 K and the same pressure are smaller than those of hcp-Fe, indicating a light element, S, reduces both density and compressional velocity of the iron inner core.

The compressional velocity and density relations for Fe_3S and hcp-Fe given in equations (2) and (3) indicate that both curves of Birch's law locate above those of the

PREM inner core. Birch's law of Fe_3S and hcp-Fe at 300 K indicates that the PREM compressional velocity of the inner core can be explained by two ways, i.e., hcp-Fe and Fe_3S have large temperature effects on Birch's law or the inner core contains heavy elements with a negligible temperature effect on Birch's law. We calculated V_S based on the equation of state of Fe_3S reported by Seagle et al. (2006) and Chen et al. (2007). The calculated V_S at the inner core is much faster than that of the PREM inner core at the inner core boundary assuming no temperature dependency in Birch's law.

Although there are some controversies in the experimental results on existence of temperature dependence on Birch's law (Antonangeli et al. 2012; Lin et al. 2005; Mao et al. 2012), recent theoretical calculations and shock wave experiments (Brown and McQueen 1981) indicate existence of large temperature dependence in Birch's law at temperatures above 2000 K. We need to determine experimentally the sound velocity at temperature above 2000 K, and the temperature dependence on Birch's law to the core conditions in order to estimate the amount of sulfur in the inner core.

Acknowledgments

The authors thank Dr Daisuke Ishikawa and Dr Hiroshi Uchiyama for their experimental assistance at BL35XU, SPring-8. They also appreciate Dr Satoru Tanaka of JAMSTEC and Dr Dapeng Zhao of Tohoku University for invaluable discussions on the seismic models of the Earth's core. S.K. gratefully acknowledges the Japan Society for the Promotion of Science for providing a research fellowship. This work was supported by JSPS KAKENHI Grant Numbers 18104009 and 22000002 awarded to E.O., and Grant Number 21740374 awarded to T.S. This work was conducted as part of the Global Center of Excellence program "Global Education and Research Center for

Earth and Planetary Dynamics". The experiments were performed under contract at SPring-8 (proposal numbers 2010A0028, 2010A1142, 2010B0028, 2010B1185, 2011A0028, and 2011A1256).

References

Antonangeli, D., Occelli, F., Requardt, H., Badro, J., Fiquet, G., and Krisch, M. (2004) Elastic anisotropy in textured hcp-iron to 112 GPa from sound wave propagation measurements. Earth and Planetary Science Letters, 225, 243–251.

Antonangeli, D., Komabayashi, T., Occelli, F., Borissenko, E., Walters, A.C., Fiquet, G., and Fei, Y. (2012) Simultaneous sound velocity and density measurements of hcp iron up to 93 GPa and 1110 K: An experimental test of the Birch's law at high temperature. Earth and Planetary Science Letters, 331–332, 210–214.

Badro, J., Fiquet, G., Guyot, F., Gregoryanz, E., Occelli, F., Antonangeli, D., and d'Astuto, M. (2007). Effect of light elements on the sound velocities in solid iron: Implications for the composition of Earth's core. Earth and Planetary Science Letters, 254, 233–238.

Baron, A. Q. R., Tanaka, Y., Goto, S., Takeshita, K., Matsushita, T., and Ishikawa, T. (2000) An X-ray scattering beamline for studying dynamics. Journal of Physics Chemistry of Solids, 61, 461–465.

Birch, F. (1961) Composition of the Earth's mantle. Geophysical Journal of the Royal Astronomical Society, 4, 295–311.

Birch, F., 1964. Density and composition of mantle and core. Journal of Geophysical Research, 69(20), 4377–4388.

Brown, J. M. and McQueen, R. G. (1986) Phase transitions, Grüneisen parameter, and elasticity for shocked iron between 77 GPa and 400 GPa. Journal of Geophysical Research, 91(B7), 7485–7494.

Campbell, A. J., Seagle, C. T., Heinz, D. L., Shen, G., and Prakapenka, V. B. (2007) Partial melting in the iron–sulfur system at high pressure: A synchrotron X-ray diffraction study. Physics of Earth and Planetary Interiors, 162, 119–128.

Cao, A., Romanowicz, B., Takeuchi, N. (2005) An observation of PKJKP: Inferences on inner core shear properties. Science, 308, 1453–1455.

Chen, B., Gao, L., Funakoshi, K., and Li, J. (2007) Thermal expansion of iron-rich alloys and implications for the Earth's core. Proceedings of the National Academy of Sciences, 104(22), 9162–9167.

Dubrovinsky, L. S., Saxena, S. K., Tutti, F., Rekhi, S., LeBehan, T., 2000. *In situ* X-ray study of thermal expansion and phase transition of iron at multimegabar Pressure. Physical Review Letters, 84(8), 1720–1723.

Dziewonski, A. M. and Anderson, D. L. (1981) Preliminary reference Earth model. Physics of Earth and Planetary Interiors, 25, 297–356.

Fei, Y., Prewitt, C. T., Mao, H.-K., and Bertka, C. M. (1995) Structure and density of FeS at high pressure and high temperature and the internal structure of Mars. Science, 268, 1892–1894.

Fei, Y., Li, J., Bertka, C. M., and Prewitt, C. T. (2000) Structure type and bulk modulus of Fe_3S, a new iron–sulfur compound. American Mineralogist, 85, 1830–1833.

Fei, Y., Ricolleau, A., Frank, M., Mibe, K., Shen, G., and Prakapenka, V. (2007) Toward an internally consistent pressure scale. Proceedings of the National Academy of Sciences, 104(22), 9182–9186.

Fiquet, G., Badro, J., Guyot, F., Requardt, H., and Krisch, M. (2001) Sound velocities in iron to 110 gigapascals. Science, 291, 468–471.

Fujihisa, H. (1999) An X-ray powder pattern analysis program for imaging plate. The Review of high pressure science and technology, 9(1), 65–70 (in Japanese).

Fujihisa, H. (2005) Recent progress in the powder X-ray diffraction image analysis program PIP. The Review of high pressure science and technology, 15(1), 29–35 (in Japanese).

Fujihisa, H., and Aoki, K. (1998) High pressure X-ray powder diffraction experiments and intensity analysis. The Review of high pressure science and technology, 8(1), 4–9 (in Japanese).

Hillgren V., Gessmann, C. K., and Li, J. (2000) An experimental perspective on the light element in Earth's core. In Canup, R. M., Righter, K., Eds., Origin of the Earth and Moon, p. 245–263. The University of Arizona, Arizona.

Kamada, S., Terasaki, H., Ohtani, E., Sakai, T., Kikegawa, T., Ohishi, Y., Hirao, N., Sata, N., Kondo, T. (2010) Phase relationships of the Fe–FeS system in conditions up to the Earth's outer core. Earth and Planetary Science Letters, 294, 94–100.

Kamada, S., Ohtani, E., Terasaki, H., Sakai, T., Miyahara, M., Ohishi, Y., and Hirao, N. (2012) Melting relationships in the Fe-Fe_3S system up to the outer core conditions. Earth and Planetary Science Letters, 359–360, 33–40.

Lin, J.-F., Fei, Y., Sturhahn, W., Zhao, J., Mao, H. K., and Hemley, R. J. (2004) Magnetic transition and sound velocities of Fe_3S at high pressure: Implications for Earth and planetary cores. Earth and Planetary Science Letters, 226, 33–40.

Lin, J.-F., Sturhahn, W., Zhao, J., Shen, G., Mao, H.-K., and Hemley, R.J. (2005) Sound velocities of hot dense iron: Birch's law revisited. Science, 308, 1892–1894.

Mao, Z., Lin, J.-F., Liu, J., Alatas, A., Gao, L., Zhao, J., and Mao, H.-K. (2012) Sound velocities of Fe and Fe-Si alloy in the Earth's core. Proceedings of the National Academy of Sciences, 109, 10239–10244.

Matsui, M. (2009) Temperature–pressure–volume equation of state of the B1 phase of sodium chloride. Physics of Earth and Planetary Interiors, 174, 93–97.

McDonough, W. F. (2003) Compositional model for the Earth's core, In R.W. Carlson Ed., Treatise on Geochemistry, p. 547–568. Elsevier, Oxford.

Ohishi, Y., Hirao, N., Sata, N., Hirose, K., and Takata, M. (2008) Highly intense monochromatic X-ray diffraction facility for high-pressure research at SPring-8. High Pressure Research, 28(3), 163–173.

Poirier J. P., 1994. Light elements in the Earth's outer core: A critical review. Physics of Earth and Planetary Interiors, 85, 319–337.

Seagle, C. T., Campbell, A. J., Heinz, D. L., Shen, G., and Prakapenka, V. B. (2006) Thermal equation of state of Fe_3S and implications for sulfur in Earth's core. Journal Geophysical Research, 111, B06209.

Seto, Y., Hamane, D., Nagai, T., and Sata, N. (2010) Development of a software suite on X-ray diffraction experiments. The Review of high pressure science and technology, 20(3), 269–276 (in Japanese).

Sha, X. and Cohen, R. E. (2010) Elastic isotropy of ε-Fe under Earth's core conditions. Geophysical Research Letters, 37, L10302.

Song X., Helmberger, D. V., 1998. Seismic evidence for an inner core transition zone. Science, 282, 924–927.

Vočadlo, L. (2007) Ab initio calculations of the elasticity of iron and iron alloys at inner core conditions: Evidence for a partially molten inner core? Earth and Planetary Science Letters, 254, 227–232.

Vočadlo, L., Dobson, D. P., and Wood, I. G. (2009) Ab initio calculations of the elasticity of hcp–Fe as a function of temperature. Earth and Planetary Science Letters, 288, 534–538.

Figure captions

Figure 1. Back scattered electron image of the synthesized Fe_3S. We can see only Fe3S in this figure and the chemical analysis using EDS showed the composition of $Fe_{73.4(0.1)}S_{26.6(0.1)}$.

Figure 2. Examples of IXS spectra taken in this study at 23.8 and 84.5 GPa. Open diamond symbols represent peak positions of TA phonons of diamond. Solid diamond symbols show peak positions of LA phonons of Fe_3S. The grey curve, grey dotted curve, grey dashed curve, and dot-dashed curve represent fitting results for Fe_3S (LA), elastic, diamond (TA) peaks, and diamond (LA) peak respectively.

Figure 3. Dispersion curves of the longitudinal acoustic phonon branch of Fe_3S at pressures from 23.8 to 84.5 GPa and room temperature.

Figure 4. V_P plotted against density. Open and solid squares represent the data of Fe_3S from this study and those from Lin et al. (2004), respectively. Solid and open upward triangles represent results of ε-Fe from Mao et al. (2012) and Antonangeli et al. (2012), respectively. Solid and open downward triangles are data of FeS reported by Vočadlo (2007) based on ab initio calculation and Badro et al. (2007) based on IXS, respectively.

Open diamonds represent data of FeS_2 reported by Badro et al. (2007). Solid diamonds are the data calculated theoretically (Vočadlo et al., 2009; Sha and Cohen, 2010). The crosses are V_P values of the PREM inner core (Dziewonsk and Anderson, 1981). The dashed line represents Birch's law for Fe_3S, and expressed by equation (2) in the text, whereas the solid line represents that for ε-Fe expressed by equation (3). Open circles are V_p of ε-Fe and Fe_3S under the core conditions with error bars. The dotted dashed line and long dash line are Birch's law for FeS_2 (Badro et al., 2007) and FeS (Badro et al., 2007; Vočadlo, 2007), respectively.

Table 1. Experimental conditions and results.

Run number	P^c [GPa]	T [K]	ρ^d [kg/m^3]	$V_P{}^e$ [m/s]
IXSFE3S03[a]	23.8(10)	300	8060(20)	6660(80)
IXSFE3S02_01[b]	35.2(35)	300	8340(20)	6950(190)
IXSFE3S04[a]	52.9(38)	300	8870(30)	7460(170)
IXSFE3S02_02[b]	55.1(16)	300	8960(10)	7650(60)
IXSFE3S07[a]	56.5(9)	300	9030(30)	7640(200)
IXSFE3S08[a]	67.4(5)	300	9200(20)	8090(270)
IXSFE3S10[c]	84.5(17)	300	9610(30)	8310(50)

The numbers in parentheses show errors. a: λ=0.41348(7) Å, b: λ=0.41495(10) Å, b: λ=0.41300(9) Å
c: The pressure was the average of multiple measurements of a sample using the equation of state of NaCl(B1) or NaCl(B2) at 300 K after annealing. The pressure error is the standard deviation of multiple measurements.
d: The density of Fe_3S was the average of multiple measurements based on XRD patterns. The density error is the standard deviation of multiple measurements. e: V_P was obtained with free Q_{MAX}

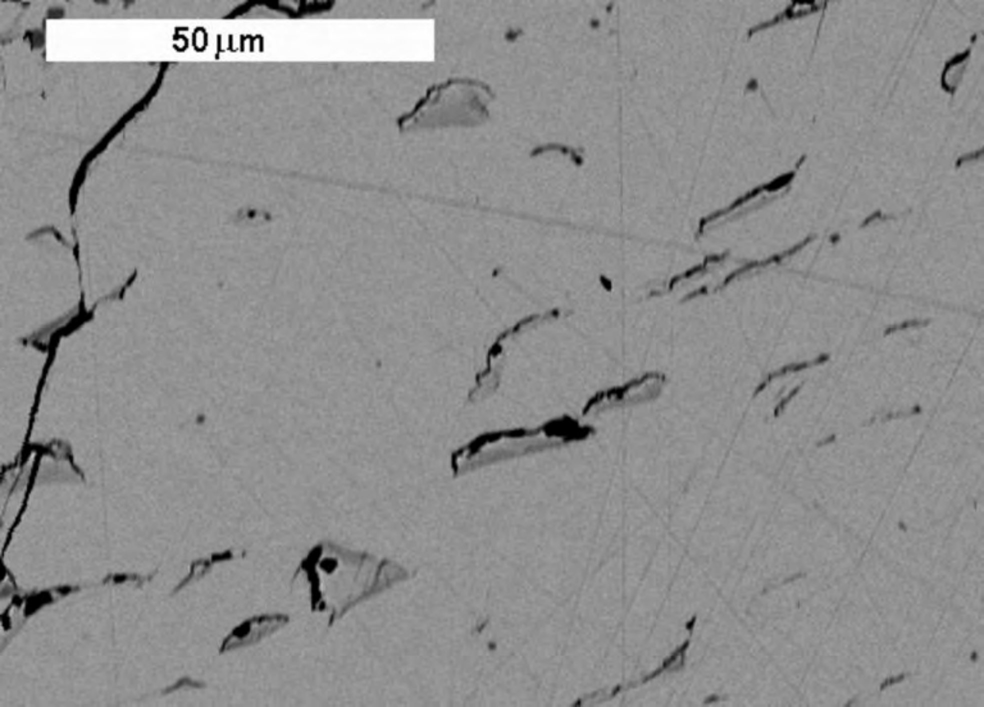
50 µm

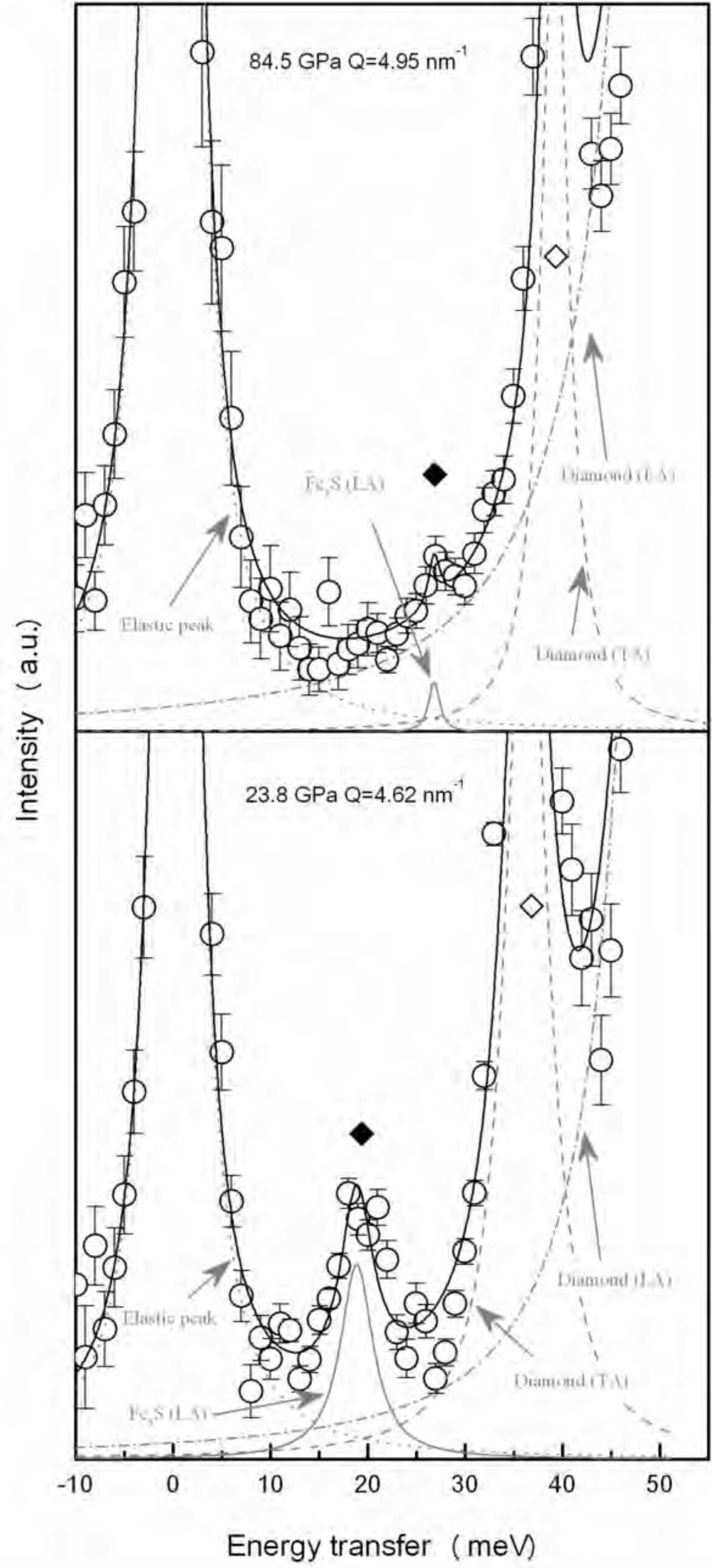

84.5 GPa Q=4.95 nm-1
Fe3S (LA)
Diamond (LA)
Elastic peak
Diamond (TA)
23.8 GPa Q=4.62 nm-1
Diamond (LA)
Elastic peak
Diamond (TA)
Fe3S (LA)
Intensity (a.u.)
-10
0
10
20
30
40
50
Energy transfer (meV)

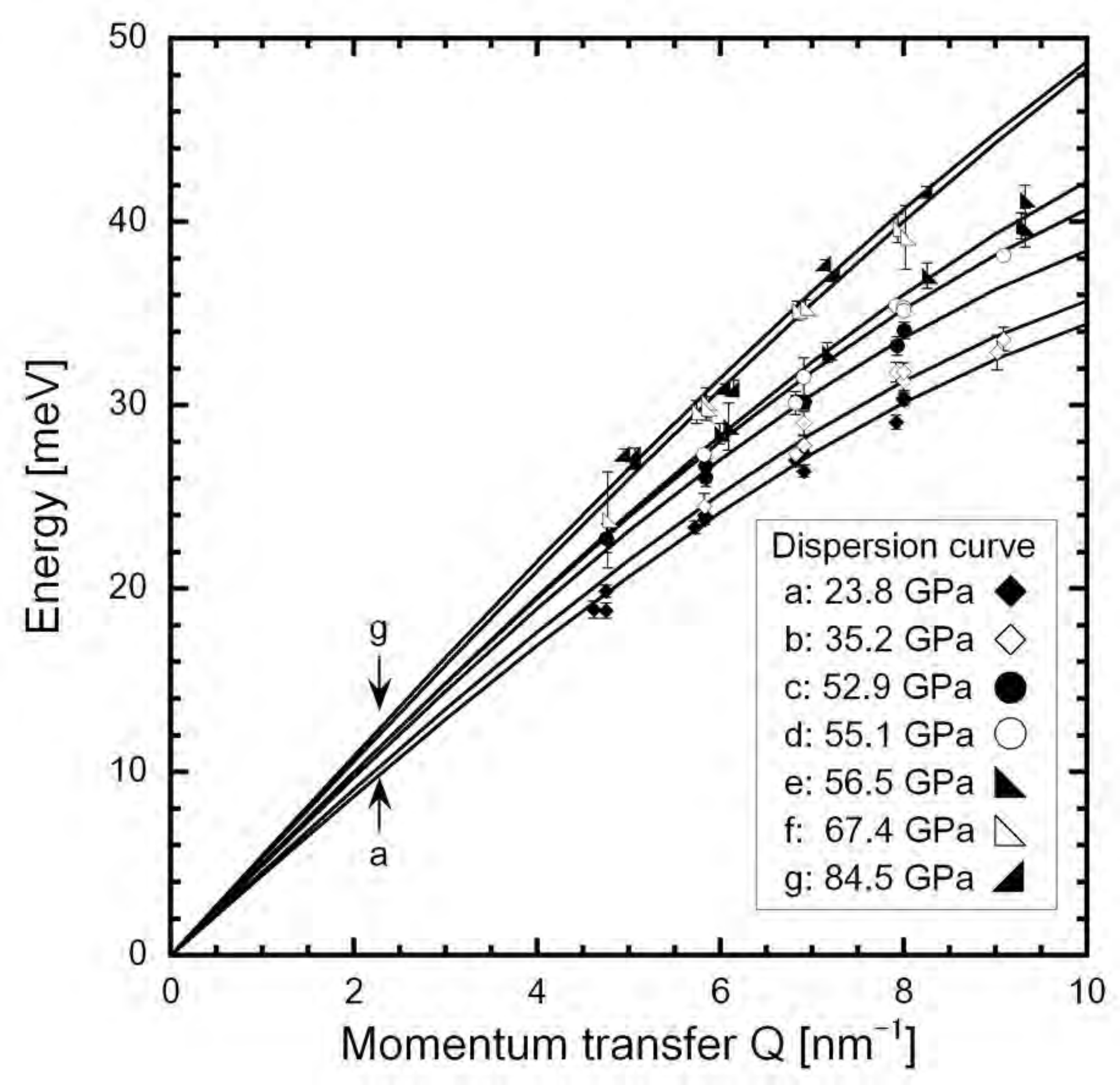

Energy [meV]
Momentum transfer Q [nm⁻¹]
0
10
20
30
40
50
0
2
4
6
8
10
g
a
Dispersion curve
a: 23.8 GPa
b: 35.2 GPa
c: 52.9 GPa
d: 55.1 GPa
e: 56.5 GPa
f: 67.4 GPa
g: 84.5 GPa

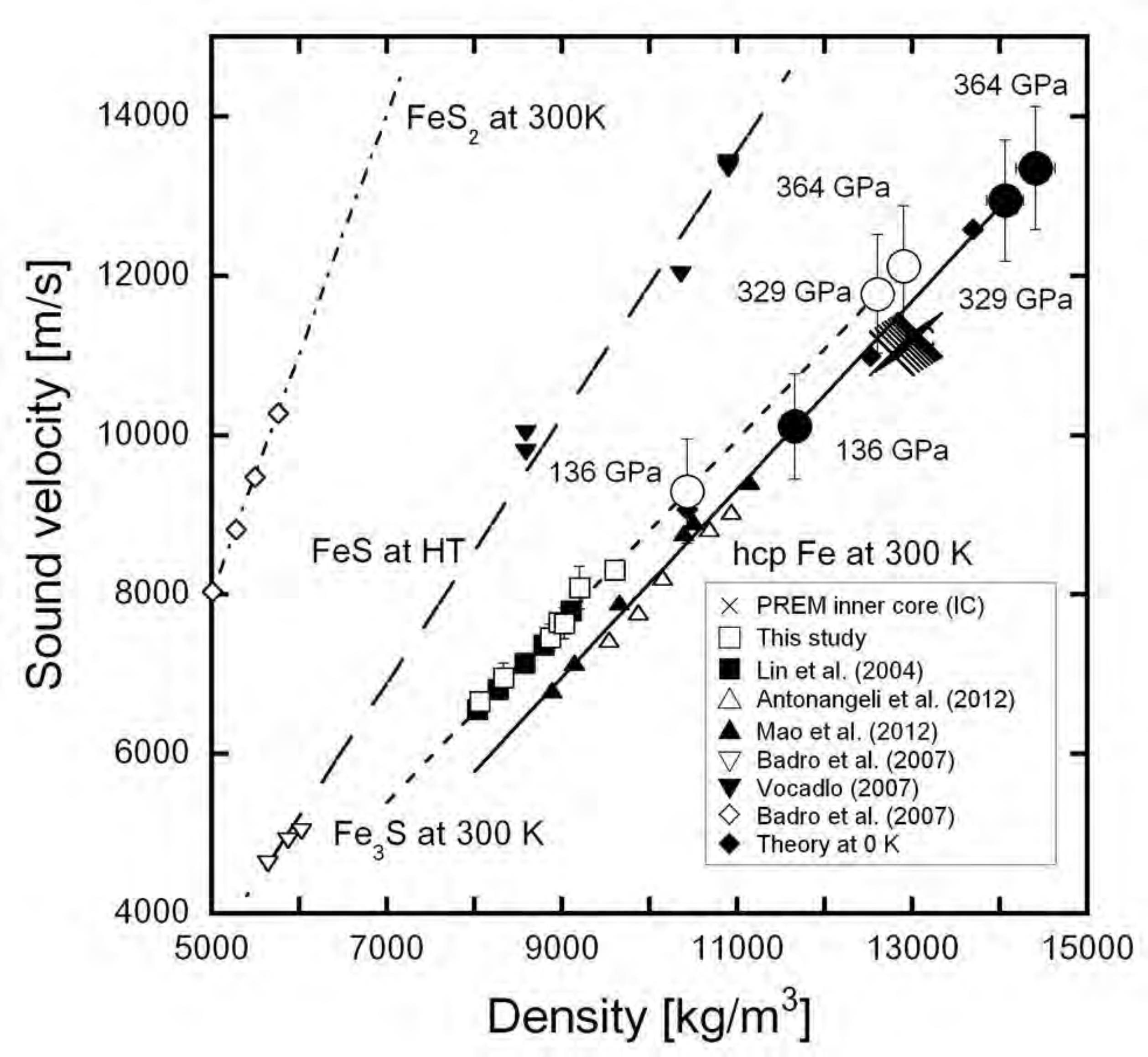

364 GPa
FeS$_2$ at 300K
364 GPa
329 GPa
329 GPa
136 GPa
136 GPa
FeS at HT
hcp Fe at 300 K
Fe$_3$S at 300 K
PREM inner core (IC)
This study
Lin et al. (2004)
Antonangeli et al. (2012)
Mao et al. (2012)
Badro et al. (2007)
Vocadlo (2007)
Badro et al. (2007)
Theory at 0 K
Sound velocity [m/s]
Density [kg/m^3]
14000
12000
10000
8000
6000
4000
5000
7000
9000
11000
13000
15000